Available online at www.worldscientificnews.com

World Scientific News

An International Scientific Journal

WSN 159 (2021) 122-144 EISSN 2392-2192

Gliricidia sepium and *Acacia* pods potential in removing depleted dyes from industrial wastewater

T. Gabriel Otusanya[1,2], O. Azeez Olajide[1,2], T. Ademola Adeniji[1,2], O. Abass Alade[1,2,3,*], J. Tinuade Afolabi[1,2]

[1]Department of Chemical Engineering, Faculty of Engineering, Ladoke Akintola University of Technology, Ogbomoso, Nigeria

[2] Bioenvironmental, Water and Engineering Research Group (BWERG), Ladoke Akintola University of Technology, Ogbomoso, Nigeria

[3]Science and Engineering Research Group (SAERG), Ladoke Akintola University of Technology, Ogbomoso, Nigeria

*Email address: aoalade@lautech.edu.ng

ABSTRACT

Biosorption of bromothymol blue from wastewater using biocomposite developed from *Gliricidia sepium* (A) and *Acacia* pods (B) was studied. The biocomposite were developed based on the Mixture Methodology of the to Design Expert software (11.0.4), where the mixed ratio was varied from 5 to 95 percentage composition and the effective mixture was evaluated based on methylene blue number (MBN) test. Adsorption capacity (AC) and Removal efficiency (RE) of the seven (7) experimental runs was studied. The surface characteristics of the materials were chemically modified and characterized using Fourier Transmission Infrared (FTIR). Batch adsorption was carried out at 10 mg/l, 15 mg/l and 20 mg/l initial concentrations at various contact time. Suitable adsorption Isotherms, kinetics models, mass transfer diffusion models and thermodynamics were studied. The RE (%) and AC (mg/g) have the highest values (96.9736 and 0.969736) at Run 3 (0.95A: 0.05B). There were appearance and disappearance of the O-H stretch, C=O, C-F, $c \equiv c$, $\equiv C$-H stretch groups in the modified and unmodified *Gliricidia sepium* at different peaks, while C-Cl stretch, C=O, N-H bend and O-H stretch groups were noticed in the modified and unmodified *Acacia* pod. The Temkin and Freundlich Isotherm represented the best fit of experimental data. The kinetic studies revealed that the pseudo-second order model fitted well. The mechanism of adsorption was controlled by Weber-Morris diffusion model. The

(Received 17 June 2021; Accepted 08 July 2021; Date of Publication 09 July 2021)

activation thermodynamic parameters were estimated. Results showed that low-cost adsorbents can be fruitfully used for the removal of dyes with a concentration range of 10-20 mg/l, it also showed that *Gliricidia sepium* and *Acacia pod* biocomposite was effective in removal of bromothymol blue from wastewater.

Keywords: Biosorption, Concentration, Bromothymol blue, Wastewater, *Gliricidia sepium*, *Acacia* Pods, Biocomposite

1. INTRODUCTION

In recent years, rapid industrialization has left impressions on the environmental society. A plethora of industries like the textile industry used dyes to colour their products, and thus produces an organic containing wastewater. In the dyeing processes, the percentage of dye lost in wastewater is 50% of the initial dye due to the low levels of dye-fibre fixation. Disposal of these dyes into effluents affects the people's usage for several purposes such as washing, bathing, and drinking. As a result of dye production industry amongst many other industries which uses dyes and pigments, wastewater generated are high both in color and organic content. About 10,000 different commercial dyes and pigments exist, and over 7×10^5 tons are produced annually world-wide. During dyeing process, approximately 10–15 % of the synthetic dyes is released into the industrial waste causing serious environmental problem [1].

Furthermore, dyes can affect aquatic plants because they reduce sunlight transmission through water [2]. Dyes also impart toxicity to aquatic life causing mutagenic, carcinogenic damages to humans, they include; kidneys dysfunction, reproductive system, liver, brain and the central nervous system. Colour removal from waste effluents had become environmentally important because even a little quantity of dye in water can be visible and toxic. Since the abatement of dyes from wastewater is regarded an environmental challenge, it is therefore essential to use treatment strategies [3], aiming to ensure the sustainability of the environment to future generations via the physical, chemical and biological means or the combination of them all [4].

Adsorption processes are being widely used by various researchers for the removal of pollutants from waste streams and activated carbon has been frequently used as an adsorbent. Activated carbon remains expensive irrespective of its extensive use in water and wastewater treatment industries. Recently, the need for safe and economical methods for the sequestration of dyes from wastewater has motivated research interest toward the production of cost effective alternatives to commercially available activated carbon. Therefore, all possible sources of agro-based inexpensive adsorbents should be explored urgently and that their feasibility for the removal of contaminants should be studied in detail.

It has been recognized that Low-cost by-products from agricultural, household and industrial sectors is a sustainable solution for wastewater treatment, and at same time, its usage contributes to minimization of waste, recovery and reuse. Despite a plethora of reviews being published in the last few years, there is inconsistencies in data presentation while using different sorbents [5].

Thus, adsorption has been preferred due to its low-cost and its high-quality of the treated effluents [6]. Adsorption by activated carbon has proven to be an effective way for wastewater treatment, however, activated carbon is associated with some restrictions such as; cost of

activated carbon and the need for regeneration after exhausting. In this present study low cost and recyclable adsorbent (Fig. 1 & 2) has been reviewed as an abatement of dye pollution from wastewater and water. It is generally a goal to replace commercial activated carbons with agricultural precursors. These agricultural precursors pose a variety of disposal problems due to their bulk volume, toxicity or physical nature (*i.e. G. sepium Acacia, Banana pills, Tangerine pills, Rice husks etc.*). If these precursors could be used as cost effective adsorbents, it will provide advantage to environmental pollution in two-fold. Firstly, by-products (or wastes) could be partly reduced and secondly the low-cost adsorbent, if developed, can reduce the pollution of wastewaters at reasonable cost [2]. The aim of this study was to effectively adsorb Bromothymol Blue from wastewater using agricultural biosorbent developed from *Gliricidia sepium* and *Acacia* pods.

Figure 1. Depiction of *Gliricidia sepium*

Figure 2. Depiction of *Acacia* seed pod

2. MATERIALS AND METHODS

2. 1. Materials

The materials used for this project work is biocomposite of *G. sepium* and *Acacia* seed pods (BGA). Some other materials that were used are Aluminium foil, Distilled water and Bromothymol Blue. The reagents that were used for this experiment are Methylene Blue, Phosphoric acid, Zinc chloride, Sodium Hydroxide.

2. 1. 1. Material Procurement and Processing

The materials were sourced in Ogbomoso town, Oyo state, Nigeria. The method used for collection of the adsorbents (*G. sepium* and *Acacia* pods) was manual i.e. picking around trees scattered throughout the university environment. The sourced material (*G. sepium* and *Acacia* pods) were sorted and then thoroughly pre-treated with a little detergent in order to kill every microbe present and remove the stains. The washing process continued until almost colourless water is observed and later washed with distilled water. After the materials were washed, they were dried continuously until a constant mass is observed when it is completely demoisturized. The dried material was crushed and milled to a 9 microns uniform particle size.

2. 1. 2. Surface Decolourization and Modification of BGA

The pre-treated materials were modified with hydrogen peroxide basically to decolorize the biosorbent and improve the surface characteristics of the material. This was carried out by dissolving hydrogen peroxide into distilled water in the ratio 1:100, the biosorbent were then brought in contact with the peroxide solution and left for 48hrs, after which it was decanted and washed off with distilled water. The process was repeated periodically every 24hrs until a clear decanted solution was observed.

2. 2. Optimization of the Biocomposite mixture of *G. sepium* and Acacia (BGA) seed pod using Methylene Number

The selected factors for the optimization of the BGA were biocomposite mix ratio of GA with range (5-95%) as shown in Figure 1. The absorbance capacity, methylene blue number, and removal efficiency were the experiments performed to determine the optimum biocomposite formulation ratio. The two-level factorial design expert software with file version (11.0.4.0) was used to generate the number of experimental runs at random for the selected factor (Table 2) and the selected responses are Adsorption Capacity and Removal Efficiency (Table 1). The design of the experiment is generally undertaken to minimize time, materials and invariably cost, involve in experimental design.

Table 1. Component Mixture.

Component	Unit	Level	
		low	High
Gliricidia sepium	%	5	95
Acacia pod	%	5	95

Table 2. Experimental design of biocomposite mix used.

Run	Gliricidia sepium (%)	Acacia (%)
1	65	35
2	5	95
3	95	5
4	35	65
5	72.5	27.5
6	50	50
7	27.5	72.5

2. 3. Fourier Transmission Infrared Spectroscopy (FTIR)

FTIR technique has been widely used for the prediction of organic compounds present in the sample by the absorption of low energy light i.e. ultraviolet light of each wavelength. The absorption spectra of the compounds are a unique reflection of the molecular arrangement of the compound in the sample. The spectrum is a graph which contains percent transmittance along Y axis and frequency or wavelength along X axis. By studying the peak between a particular frequency i.e., gap or band, type of the functional group present was predicted with the help of available table [7]. This analysis was performed individually for the modified and unmodified GA.

2. 4. Batch Adsorption of Bromothymol Blue from wastewater onto BGA

Effect of adsorbate concentration being a factor that affects the adsorption of bromothymol blue on BGA was studied. The parameters – Adsorption Capacity (AC) in mg/g and Removal Efficiency (RE) – of the factor studied was also evaluated using equation 1 and 2.

$$AC = \frac{(Co - Ce)V}{W} \quad (1)$$

$$RE = \frac{C_o - C_e}{C_o} \times 100\% \quad (2)$$

where: Co and Ce are the concentrations (mg/L) of the dye initially and at equilibrium time, V is the volume of the adsorbate and W is the weight of the adsorbent [8].

3. RESULT AND DISCUSSION

3. 1. Optimization of the Biocomposite mixture of *G. sepium* and *Acacia* (BGA) seed pod using Methylene Number

The experimental design data for adsorption capacity (mg/g) and removal efficiency (%) gives the following results (Table 3). Suitable models for adsorption capacity and removal efficiency were usually selected based on the highest order polynomials. The Quartic model has the highest R^2 value (0.9999) and lowest standard deviation (0.0010) for the adsorption capacity while in Removal efficiency the Cubic model has the highest R^2 value (1.0000) and lowest standard deviation (0.0096). The suitability of the model was further supported with the least value (0.0138) of the Predicted Residual Error Sum of Squares (PRESS) for the adsorption capacity, while that of removal efficiency has a PRESS value of 0.0347. The positive and negative coefficients indicated positive and negative influences of the independent variables on the selected responses.

Table 3. Model Summary Statistics for Adsorption Capacity and Removal Efficiency.

Adsorption Capacity					
Source	**Sequential p-value**	**Adjusted R²**	**Std. Dev.**	**R²**	**PRESS**
Linear	0.1960	0.2192	0.0341	0.3753	0.0180
Quadratic	0.1269	0.5778	0.0251	0.7467	0.0139
Cubic	0.6361	0.4506	0.0286	0.7802	0.5479
Quartic*	0.0162	0.9993	0.0010	0.9999	0.0138
Removal Efficiency					
Source	**Sequential p-value**	**Adjusted R²**	**Std. Dev.**	**R²**	**PRESS**
Linear	0.0941	0.5486	0.5119	0.6615	3.60
Quadratic	0.0741	0.9034	0.2368	0.9517	3.09
Cubic*	0.0182	0.9998	0.0096	1.0000	0.0347

*Suggested Results are means of duplicate

3. 2. ANOVA of Adsorption capacity (Cubic model) and Removal Efficiency (Quartic model)

The analysis of variance (ANOVA) procedure was used to determine the significance of variables and to substantiate the adequacy of the quadratic regression model obtained in this study. The significance of the model was based on the principle of the Fisher's statistical test (F-test) and it generates the F-value, which represents the ratio of the mean square of regression to the mean error. Significance of the model terms were further tested based on lower probability (p-value) which may lie between 90 % confidence level [9]. Lack of fit, which is usually preferred to be insignificant, was also used as diagnostic test to determine the adequacy of any model developed [10]. The results of the ANOVA are presented in Table 4. The Mixture Component coding is L_Pseudo for adsorption capacity and removal efficiency.

Sum of squares is Type III – Partial. The Model F-value for adsorption capacity and removal efficiency are 1766.28 and 8446.28 respectively. These values imply there are 1.78% and 0.80% chances that an F-value this large could occur due to noise. P-values less than 0.0500 indicate model terms are significant. In this case A, B, $AB(A-B)^2$ are significant model terms. Values greater than 0.1000 indicate the model terms are not significant. If there are many insignificant model terms (not counting those required to support hierarchy), model reduction may improve your model.

Table 4. A NOVA for Response Surface model Analysis for adsorption capacity.

Source	Adsorption Capacity				Removal Efficiency			
	Sum of Squares	Mean Square	F-value	p-value	Sum of Squares	Mean Square	F-value	p-value
Model	0.0075	0.0019	1766.28	0.0178	2.3200	0.774	8446.28	0.0080
[(1)]Linear Mixture	0.0028	0.0028	2652.12	0.0124	1.5400	1.540	16761.38	0.0049
AB	0.0006	0.0006	596.44	0.0261	0.6438	0.643	7024.29	0.0076
AB(A-B)	0.0011	0.0011	1025.40	0.0199	0.1121	0.112	1222.61	0.0182
Residual	1.055E-06	1.055E-06			0.0001	0.001		
Cor. Total	0.0075				2.3200			

P> 0.10 A - *G. sepium* B – *Acacia* Pod

3. 3. Fit Statistics for adsorption capacity and removal efficiency

Table 5. Statistics for Adsorption Capacity and Removal Efficiency.

	Adsorption Capacity	Removal Efficiency
Properties	Values	Values
Std. Dev.	0.0010	0.0096
Mean	1.16	95.62
C.V. %	0.0887	0.0100
R^2	0.9999	1.0000
Adjusted R^2	0.9993	0.9998

Predicted R^2	-0.8570	0.9851
Adeq Precision	129.4540	210.8337

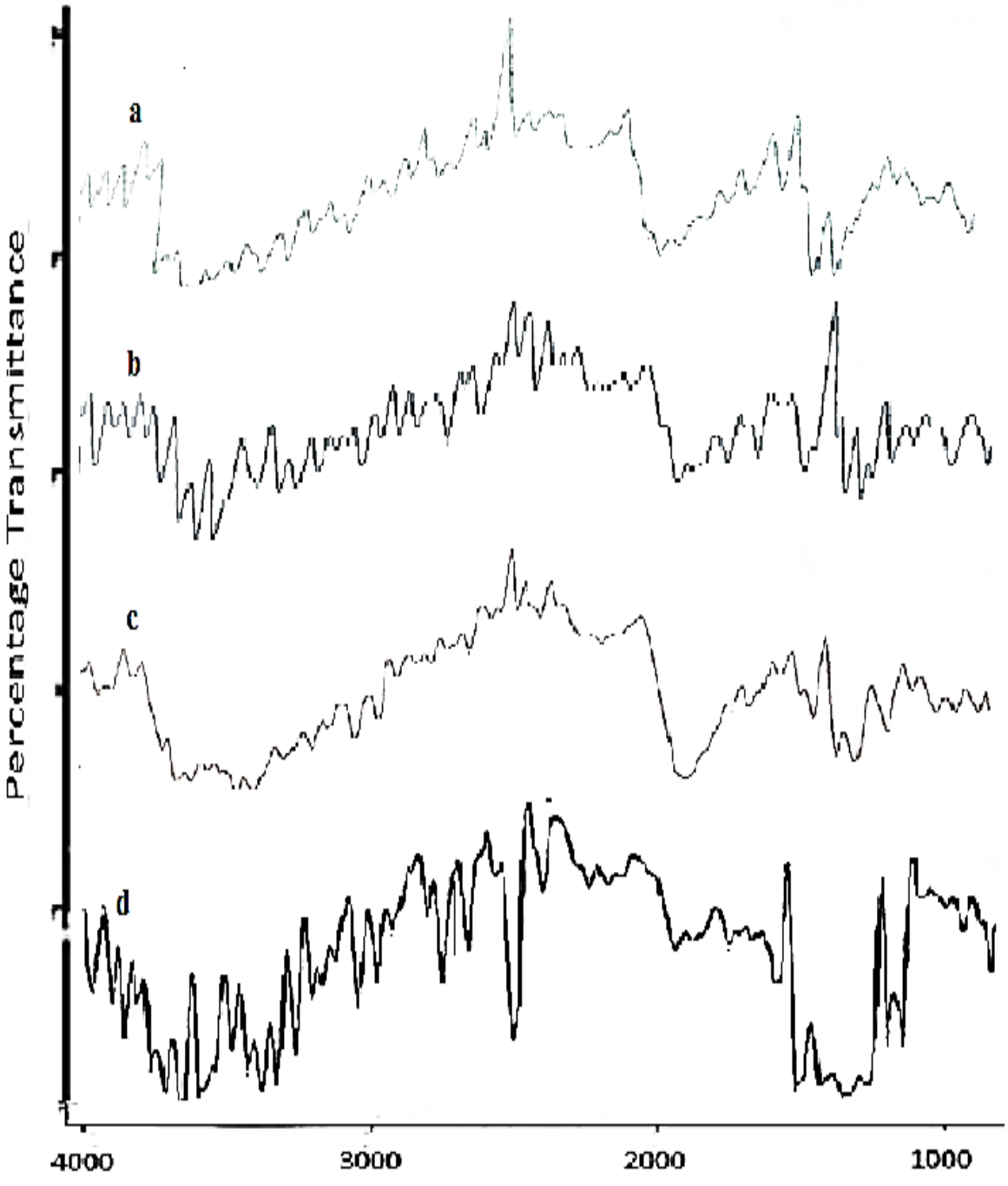

Figure 3. FTIR spectra of **(a)** *Gliricidia sepium* unmodified, **(b)** *Gliricidia sepium* modified **(c)** *Acacia* unmodified, **(d)** *Acacia* modified.

The adsorption capacity negative Predicted R^2 of -0.8570 implies that the overall mean may be a better predictor of your response than the current model. In some cases, a higher order model may also predict better. While for removal efficiency, a positive Predicted R^2 0.9851 is close to the Adjusted R^2 of 0.9998 which is what one normally expect; i.e. the difference is not greater than 0.2 (Table 5). It may indicate a large block effect or a possible problem with your model and/or data if the difference is greater than 2. Things to consider are model reduction, response transformation, outliers, etc. All empirical models should be tested by doing confirmation runs. Adeq Precision measures the signal to noise ratio. A ratio greater than 4 is desirable. The ratio of adsorption capacity and removal efficiency are 129.454 and 210.834 respectively, these values indicate an adequate signal. These models can be used to navigate the design space.

3. 4. Fourier Transform Infrared Spectroscopy (FTIR)

The presence of various functional groups presents on the surface of the adsorbent and their role in adsorption was analysed using FTIR (Fourier Transform Infrared) spectrum within the range of 400–4000 cm^{-1} using Thermo-Fisher FTIR analyser (SCIENTIFIC, NICOLET 5700). The presence of these functional groups in the activated carbon is responsible for adsorption for different heavy metal from aqueous solution [11]. The FTIR of *G. sepium* unmodified, *G. sepium* modified, Acacia unmodified and Acacia modified are presented in Figure 3a - d respectively. The IR peak (Figure 3a) observed in the *G. sepium* unmodified ranges from 612.2 to 3957.6 cm^{-1} while that of the modified (Figure 3b) ranges from 609.5 to 3964.2 cm^{-1}. In Acacia pod, it was observed that the unmodified IR peak (Figure 3c) ranges from 636.6 - 3964.2 cm^{-1} while the IR peak for the modified (Figure 3d) ranges from 610.2 - 3964.1 cm^{-1}. Some changes were observed in the functional groups of both samples as there was appearance of the C= stretch at peak of 5.7 cm^{-1} and O-H stretch at peak of 5.7 cm^{-1} after the modification of *G. sepium* . It was also observed that in Acacia there was an appearance of the N-H stretch at peak height of 4.1 cm^{-1} and C-O stretch at a peak height of 5.9 cm^{-1}. The FTIR helped to reveal whether a reduction, appearance, disappearance or broadening of the peaks after the modification with hydrogen peroxide has occurred by the spectrum of the sample [12].

3. 5. Effect of concentration on the adsorption BB on modified GAB

3. 5. 1. QE and RE Study

Effect of initial concentration of the adsorbate has a great influence in the adsorption process using modified GAB. The effect of initial concentration of the BB at various time from 15 minutes to 210 minutes were investigated for concentration 10 mg/l, 15 mg/l and 20 mg/l. It appeared that at an increasing time from 15- 210 minutes the adsorption capacity increased (Figure 4). Also, adsorption capacity increased with increasing initial concentration of the BB dye. The maximum adsorption capacity for all concentration were observed to occur at 210 minutes and the values are estimated to be 0.819767 mg/g, 1.267442 mg/g, and 1.639535 mg/g for 10 mg/l, 15 mg/l and 20 mg/l respectively. The lowest adsorption capacities were observed to occur at 15 minutes with the data estimated as 0.491279 mg/g, 0.94186 mg/g and 1.34593 mg/g for 10 mg/l, 15 mg/l and 20 mg/l. The trend from the adsorption capacity results from studied concentrations shows that adsorption capacity increases with increase in initial concentration and it agrees with results in a similar study by Amuda *et al*., (2013). Removal efficiency has been greatly affected by initial concentration of the dye during adsorption

process. The removal efficiencies were observed to increase with an increase in time from 15-210 minutes also with an increase initial concentration across 10 mg/l, 15 mg/l and 20 mg/l (Figure 4). The maximum experimented RE for all concentrations were calculated to be 82%, 84% and 82% for 10 mg/l, 15 mg/l and 20 mg/l, respectively. The lowest removal efficiency for concentration 10 mg/l, 15 mg/l and 20 mg/l are 49%, 63% and 67% respectively. The trend from these results shows that increase in initial concentration of the dye increases the removal efficiency of the adsorbate and it is in consonance with previous study by Latinwo *et al*., (2015) [13].

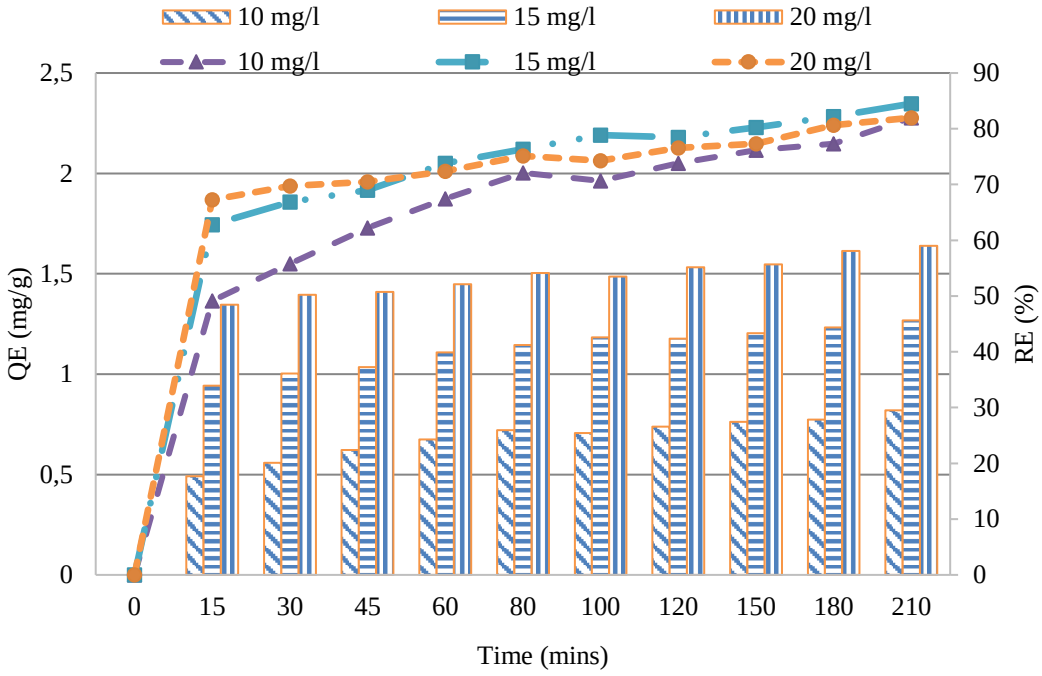

Figure 4. Effect of concentration on the adsorption of BB on modified BAG.

3. 5. 2. Isotherms Study

Langmuir

From the Langmuir linear isotherm model [14], Ce/qe was plotted against Ce to get a straight-line curve with a slope of 1/qm and intercept of $1/K_Lq_m$. Langmuir constants were derived from the plot of the isotherm (Figure 5a) and presented in Table 6. The graphical plot of Langmuir model gave R^2 values of 0.9017, 0.9376 and 0.9684 for concentration 10 mg/l, 15 mg/l and 20 mg/l respectively. The estimated isotherm parameters of qm are -10.0100 mg/g, -9.1743 mg/g and -11.9190 mg/g for 10 mg/l, 15 mg/l and 20 mg/l concentrations respectively. The estimated b or K_L values are 0.1777, -0.1938 and -0.1144 mg/l for concentration 10 mg/l, 15 mg/l and 20 mg/l respectively. The R^2 values which shows how fitted the statistical data are to the regression line, when compared to R^2 from Freundlich (0.9496, 0.9736 and 0.9858), Temkin (0.9761, 0.9849, 0.9919) and Harkins-Jura (0.8729, 0.9427, 0.9682) shows that the Langmuir model didn't show a better fit compared to other isotherm models studied on effect of concentration which suggests that the adsorption of BB on modified BAG cannot be fully describe to be monolayer adsorption process.

Freundlich

Freundlich isotherm model assumes heterogeneous adsorbent surface with its adsorption sites varying energy level [15], [30]. The plot of ln qe against lnC_e (Figure 5b) gave a straight line used in determining the Freundlich parameters which is the R^2, intercept 1/n and slope K_f (Freundlich constant) and e is the adsorption capacity at equilibrium (mg/g) (Table 6). The graphical plot of the Freundlich model gave R^2 values of 0.9496, 0.9736, 0.9858 for concentration 10 mg/l, 15 mg/l and 20 mg/l respectively. This shows a better fit compared to Langmuir isotherm (0.9017, 0.9376, 0.9684) and Harkins-Jura isotherm (0.8729, 0.9427, 0.9682). The estimated isotherm parameter K_f is -0.6126, -0.7129, 0.7209 for concentration 10 mg/l, 15 mg/l and 20 mg/l respectively. The estimated values for the parameter 1/n for concentration 10 mg/l, 15 mg/l and 20 mg/l are 0.1504, 0.5484 and 0.9249, respectively. A favorable adsorption process is obtained when 1/n lies between 0 and 1. This indicates strong interaction between the adsorbate and the adsorbent as well as the heterogeneous process [16]. The 1/n obtained from the study gives a favorable biosorption process and this compared well with a related study by Saikaew *et al*., (2009) with value of 2.5303 [17].

Temkin

The Temkin isotherm model accounts for the adsorbent-adsorbate interaction [18]. The plot fractional coverage Θ against lnCe (Figure 5c) to get slope and intercept used to evaluate the Temkin isotherm parameters K_o and RT/ΔQ. The RT/ΔQ values estimated are -0.3187, -0.3786 and -0.4898 for the concentration 10 mg/l, 15 mg/l and 20 mg/l concentrations respectively. The K_o values estimated are 0.0387, 0.0540 and 0.0732 for 10 mg/l, 15 mg/l and 20 mg/l respectively. The R^2 values obtained from the Temkin model are 0.9761, 0.9849, 0.9919 for concentration 10 mg/l, 15 mg/l and 20 mg/l respectively. This shows the best fit compared to R^2 from Langmuir (0.9017, 0.9376, 0.9684), Freundlich (0.9496, 0.9736, 0.9858) and Harkins-Jura isotherm model (0.8729, 0.9427, 0.9682).

Harkins-Jura (H-J)

H-J model [19] is described by the plot of 1/qe against log Ce (Figure 5d) and its estimated parameters are R^2, A, and B. The estimated R^2 values are 0.8729, 0.9427 and 0.9682 for concentration 10 mg/l, 15 mg/l and 20 mg/l respectively. The R^2 values is lesser than that of Langmuir (0.9017, 0.9376, 0.9684), Freundlich (0.9496, 0.9736, 0.9858), and Temkin (0.9761, 0.9849, 0.9919) which means it's not suitable since it doesn't show a better fit compared to others. The estimated parameter A and B are deduced as -0.1783, -0.7696, -1.4743 for A and 0.0699, -0.0657 and -0.0293 for B with concentration 10 mg/l, 15 mg/l and 20 mg/l respectively.

Dubinin-Radushkevich

Dubinin-Radushkevich isotherm model [20] is described by the plot of Lnqe against $Ɛ^2$ (Figure 5e). The parameter estimated from the plots are R^2, B and q_m. The correlation coefficient R^2 obtained from this model for concentration 10 mg/l, 15 mg/l and 20 mg/l are 0.7849, 0.8661, 0.9282 respectively. Other studied isotherm model Langmuir (0.9017, 0.9376, 0.9684), Freundlich (0.9496, 0.9736, 0.9858), Temkin (0.9761, 0.9849, 0.9919), Harkin-Jura (0.8729, 0.9427,0.9682), Fowler-Guggenheim (0.9879, 0.9901, 0.9947), Hill-de Boer (0.9478, 0.9613, 0.9802) and Halsey (0.9496, 0.9736, 0.9856) fit better compared to Dubinin isotherm model but Kiselev (0.6742, 0.8067,0.8996) model fits poorly. The parameter B obtained for

concentration 10 mg/l, 15 mg/l and 20 mg/l are -5E-7, -5E-7 and -8E-7 respectively. Maximum adsorption capacity q_m for the Dubinin isotherm model are 0.5176, 0.9298 and 1.2611 for concentration 10 mg/l, 15 mg/l and 20 mg/l respectively.

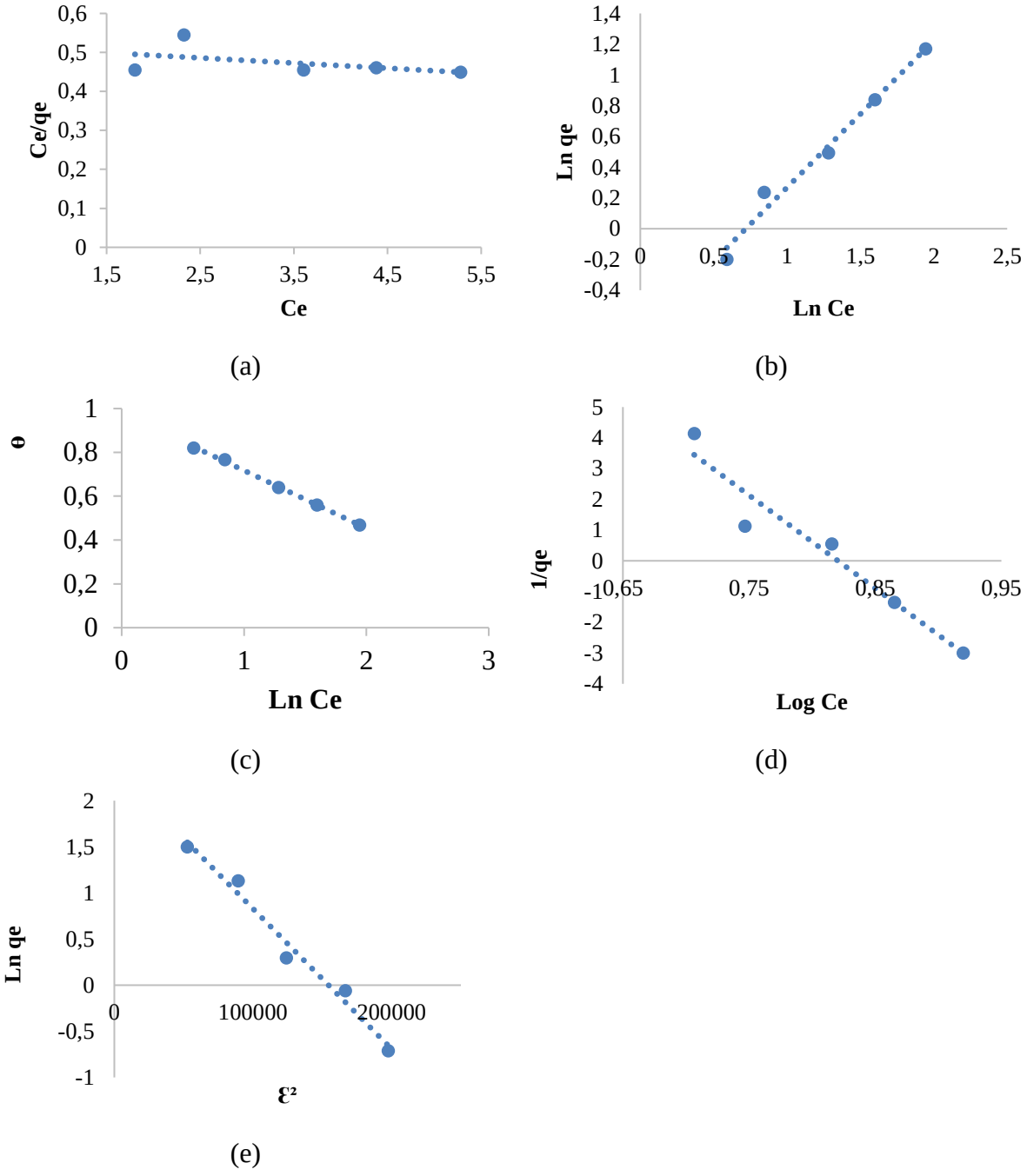

Figure 5. (a) Langmuir (b) Freundlich (c) Temkin (d) Harkins- (d) Hill-de Boer (e) Dubinin-Radushkevich Isotherm models of the adsorption of BB on modified BAG

Table 6. Isotherms model estimated parameters.

Isotherms	Parameters	Concentration		
		10 mg/l	15 mg/l	20 mg/l
Langmuir	R^2	0.9017	0.9376	0.9684
	Q_m (mg/g)	-10.0100	-9.1743	-11.9190
	b or K_L (mg/g)	0.1777	-0.1938	-0.1144
Freundlich	R^2	0.9496	0.9736	0.9858
	K_f (mg/g)	-0.6126	-0.7129	-0.7209
	1/n	0.1504	0.5484	0.9249
Temkin	R^2	0.9761	0.9849	0.9919
	K_o (L/g)	0.0387	0.0540	0.0732
	RT/ΔQ	-0.3187	-0.3786	-04896
Harkins jura	R^2	0.8729	0.9427	0.9682
	A	-0.1783	-0.7696	-1.4743
	B	0.0699	-0.0657	-0.0293
Dubinin-Radushkevich	R^2	0.7849	0.8661	0.9282
	B	-5exp-7	-5exp-7	-8exp-7
	Q_m (mg/g)	0.5176	0.9298	1.2611

3. 5. 3. Kinetics Study on effect of Concentration

Pseudo-First Order Kinetic models

The plot of ln (Q_e-Q_t) against time in describes the relationship between the pseudo-first order kinetics [21]. constant as obtained from the slope and intercept of the plot for 10 mg/l, 15 mg/l and 20 mg/l (Figure 6a) and presented in Table 7. The kinetic parameter for each of the concentration obtained are K_1, q_e cal, q_e experimental and R^2. The qe cal parameter from are estimated to be 0.3350, 0.3780 and 0.3960 for the concentration 10 mg/l, 15 mg/l and 20 mg/l respectively. The qe experimental parameter obtained are 0.819767, 1.267442 and 1.639535 for concentration 10 mg/l, 15 mg/l and 20 mg/l respectively. It is generally observed that there is a variation between the qe cal and the qe exp for all the concentration; as such, it indicates that pseudo-first order poorly fits the data. The K_1 values estimated are 0.0117, 0.0129, 0.0122 for concentration 10 mg/l, 15 mg/l and 20 mg/l respectively. The estimated R^2 parameter are

0.9550, 0.9730, 0.8699 for concentration 10 mg/l, 15 mg/l and 20 mg/l respectively. The R^2 values are less than that of Pseudo-second order (0.9968, 0.9986, 0.9977) and Elovich (0.9936, 0.9933, 0.9964) which buttress the point that it is a poorly fit data.

Pseudo-Second Order Kinetic models

The plot of t/q against t was used to evaluate K_2, qe exp, qe cal and R^2 for the pseudo-second order model [22] equation parameters (Figure 6b). The K_2 obtained for 10 mg/l, 15 mg/l and 20 mg/l concentrations are 0.0932, 0.0782 and 0.0766 respectively. The qe cal parameters were estimated to be 0.8540, 1.3016 and 1.6653 for the concentration 10 mg/l, 15 mg/l and 20 mg/l respectively. The qe experimental parameter obtained are 0.819767, 1.267442 and 1.639535 for concentration 10 mg/l, 15 mg/l and 20 mg/l respectively. The closeness between the qe cal and qe exp for both concentration and this suggests that pseudo-second order fitted the adsorption data better than Pseudo-first order. The estimated R^2 parameter for the model is 0.9968, 0.9986, 0.9977. The R^2 values is well fitted compared to Pseudo-first order (0.9550, 0.9730, 0.8699) and Elovich (0.9936, 0.9933, 0.9964). High R^2 values obtained for pseudo-second order further emphasizes the suitability over pseudo-first order and Elovich model.

Elovich model

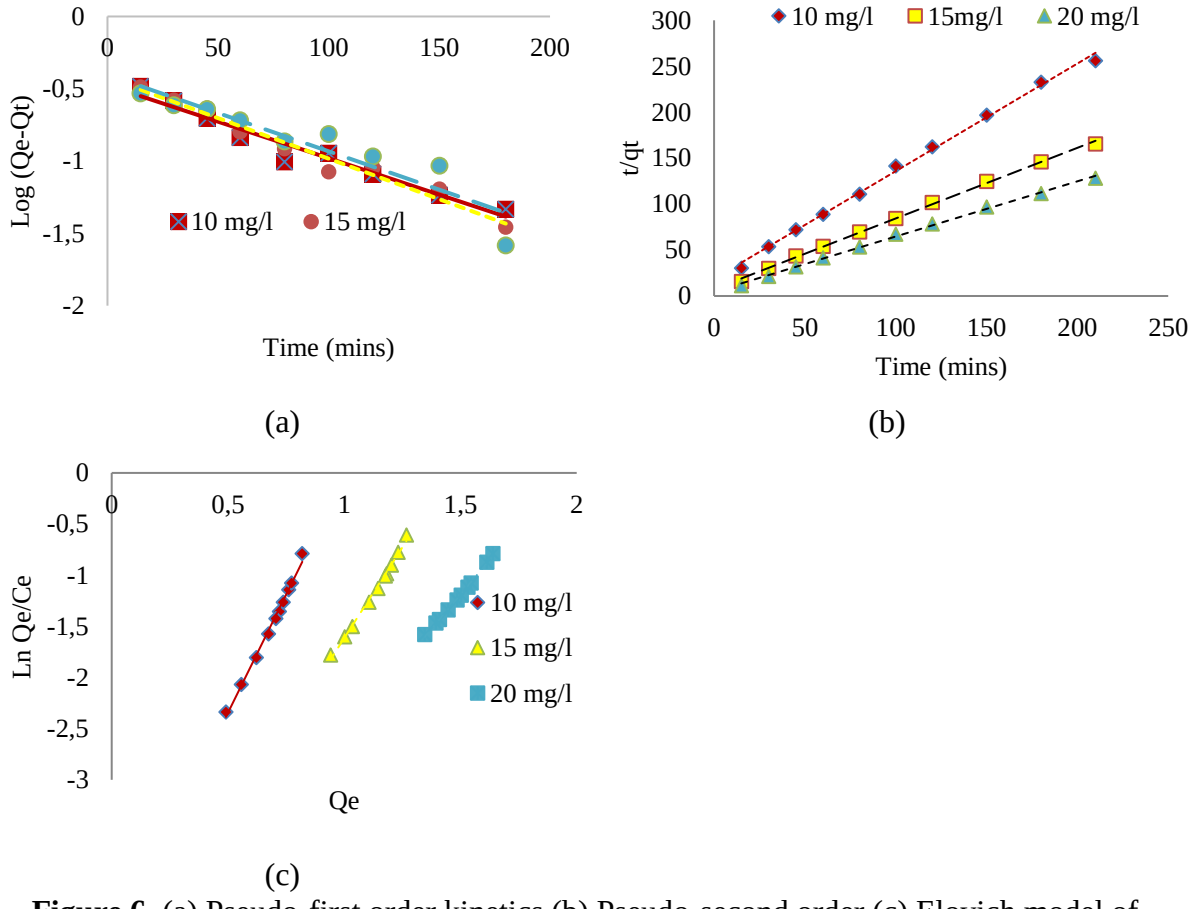

Figure 6. (a) Pseudo-first order kinetics (b) Pseudo-second order (c) Elovich model of the adsorption of BB on modified BAG

The plot of ln q_e/C_e against qe in describes the relationship between the Elovich model [23] kinetic constant as obtained from the slope and intercept of the plot for 10 mg/l, 15 mg/l and 20 mg/l (Figure 6c). The kinetic parameter for each of the concentration obtained are K_E, qm and R^2. The qm parameter are -0.2166, -0.2819, -0.9964 for concentration 10 mg/l, 15 mg/l and 20 mg/l respectively. The K_E parameters were estimated to be -0.0440, -0.0203 and -0.0144 for concentration 10 mg/l, 15 mg/l and 20 mg/l respectively. The correlation coefficient R^2 for the Elovich model is estimated to be 0.9936, 0.9933, 0.9964 for concentration 10 mg/l, 15 mg/l and 20 mg/l respectively. The R^2 values are well fitted compared to the pseudo-first order kinetic model values (0.9550, 0.9730, 0.8699).

3. 5. 4. Mass Transfer Diffusion study on effect of Concentration

Dumwald-Wagner diffusion model [24]

The plot of log ($1-F^2$) against time (t) gives a linear plot. The Dumwald-Wagner rate constant K and R^2 values for 10 mg/l, 15 mg/l and 20 mg/l concentrations were evaluated from the slope (Figure 7a). The K parameters estimated are 0.0138, 0.0177 and 0.0187 for concentration 10 mg/l, 15 m/l and 20 mg/l respectively. The R^2 values estimated for the concentration 10 mg/l, 15 mg/l and 20 mg/l are 0.8345, 0.7127 and 0.4518 respectively. The R^2 values obtained are less than values obtained from Weber Morris diffusion model (0.9327, 0.9575 and 0.9751). The linear plot intersected at the origin, and this implies that film diffusion is involved in the mechanism of the biosorption process [26].

Weber Morris diffusion model [25]

The determination of the intraparticle diffusion constants was achieved through the intercept and slope of the plot Qe against $T^{0.5}$. The estimated constants K_{wm} (intraparticle diffusion constant), C (intercept) and R^2 are obtained from the slope and intercept. The R^2 values obtained from the model at various concentrations of 10 mg/l, 15 mg/l and 20 mg/l are 0.9327, 0.9575 and 0.9751 respectively (Figure 7b). The R^2 values obtained are well fitted compared to Dumwald-Wagner (0.8345, 0.7127, 0.4518). The intercept C values obtained for concentration 10 mg/l, 15 mg/l and 20 mg/l are 0.4204, 0.8499 and 1.2399, respectively. The intercept gotten from the plot increased as the concentration increases from 10 mg/l to 15 mg/l, and this indicates that biosorption process had a boundary layer effect [13]. The study indicates increasing intercept value as concentration increases indicates that the biosorption process is more of a boundary surface (film) diffusion. The intraparticle diffusion constant Kwm were estimated to be 0.0284, 0.0298 and 0.0268 for concentration 10 mg/l, 15 mg/l and 20 mg/l respectively. The linear plot did not pass through the origin, and this indicates that intraparticle diffusion is not the sole rate-determining step [26].

Banghams diffusion model [27]

The plot of $\log log \frac{Co}{Co-qt.m}$ against log t gives a linear plot (Figure 7c). The Banghams constant K_B, Θ and R^2 values for 10 mg/l, 15 mg/l and 20 mg/l concentrations were evaluated from the slope and intercept. Correlation coefficient values obtained from the evaluation are 0.7962, 0.8589, 0.9568 for concentration 10 g/l, 15 mg/l and 20 mg/l respectively. Parameter K_B were estimated to be 5.6337, 6.7748 and 7.0193 for concentration 10 g/l, 15 mg/l and 20 mg/l respectively while parameter Θ was estimated for the varied concentration to be 0.001,

0.0006 and 0.0004. R^2 values obtained shows a better fit compared to studied model Mc Kay (0.4062, 0.1428, -0.278), Dumwald (0.8345, 0.7127, 0.4518) and Vermeulin (0.8345, 0.7127, 0.4518) but Weber Morris diffusion model (0.9327, 0.9575 and 0.9751) fits the data best on the regression line.

Vermeulen diffusion model [28]

The plot of -ln $\left(1-\left(\frac{qt}{qe}\right)^2\right)$ against time was used to evaluate K_v and R^2 for the Vermeulin diffusion model parameters (Figure 7d). The estimated constant Kv for the varied concentration (10 mg/l, 15 mg/l and 20 mg/l) are 0.0139, 0.0176 and 0.0187 respectively. Correlation coefficient R^2 obtained at varied concentration of 10 mg/l, 15 mg/l and 20 mg/l are 0.8345, 0.7127 and 0.4518 respectively. It was observed that the R^2 values obtained from Vermeulen model correlates at all concentration with obtained R^2 from Dumwald-Wagner model. This depicts that the data fits better compared to Mc Kay diffusion model (0.4062, 0.1428, -0.278).

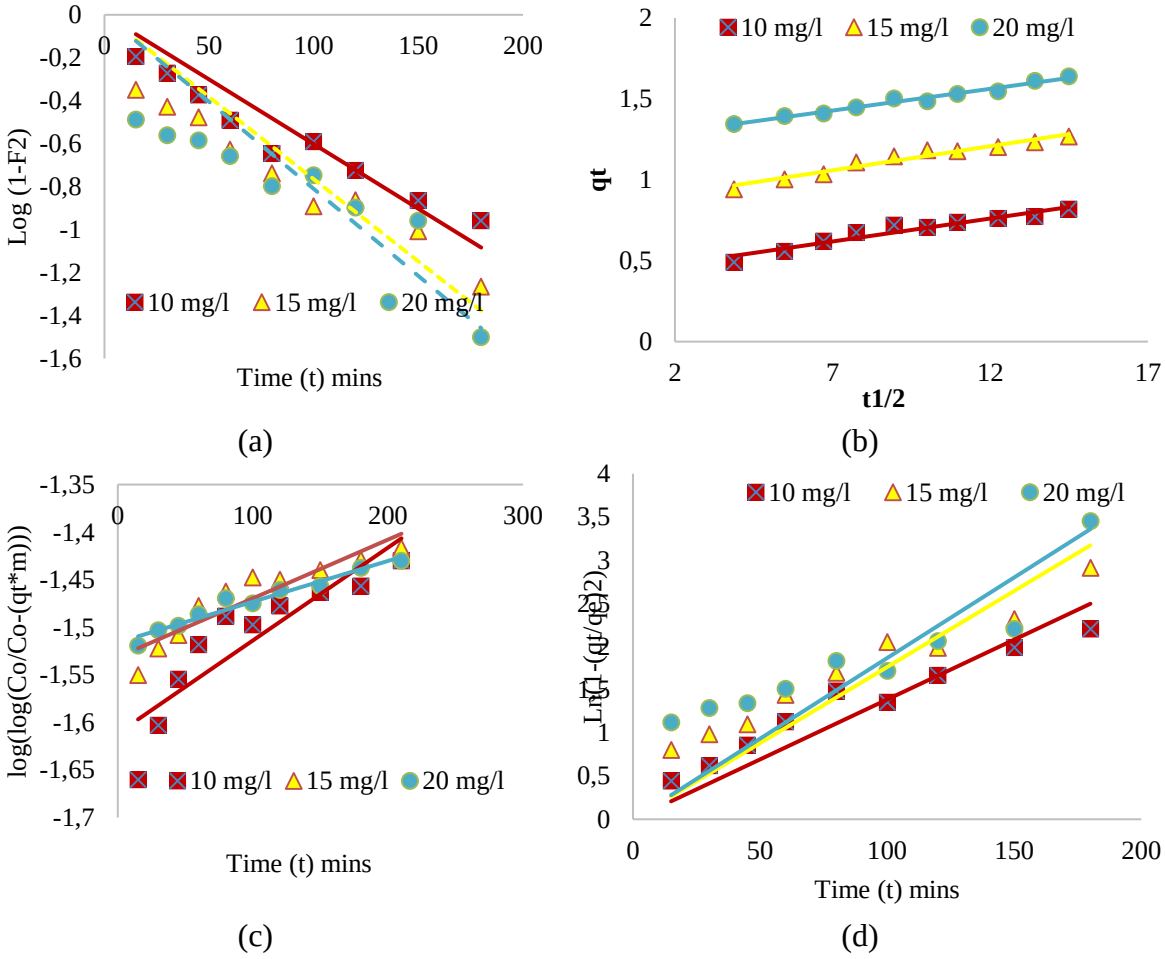

Figure 7. (a) Dumwald-Wagner diffusion model (b) Intraparticle diffusion (Weber Morris) (c) Banghams (d) Vermeulin diffusion model of the adsorption of BB on modified GAB

Table 7. Kinetics estimated parameters for effect of concentration.

Kinetics	Parameters	Concentration		
		10 mg/l	**15 mg/l**	**20 mg/l**
Pseudo 1st Order	R^2	0.9550	0.9730	0.8699
	K_1 (min^{-1})	0.0117	0.0129	0.0122
	Q_e (mg/g)	0.3350	0.3780	0.3960
Pseudo 2nd Order	R^2	0.9968	0.9986	0.9977
	K_2 (mg/g.min^{-1})	0.0932	0.0782	0.0766
	Q_e (mg/g)	0.8540	1.3016	1.6653
Elovich	R^2	0.9936	0.9933	0.9964
	Q_m (mg/g)	-0.2166	-0.2819	-0.3709
	K_E (mg/g)	-0.0440	-0.0203	-0.0144

3. 6. Thermodynamic Study

Table 8. Mass transfer diffusion models calculated parameters for effect of concentrations.

Mass transfer	Parameters	Concentration		
		10 mg/l	**15 mg/l**	**20 mg/l**
Weber Morris (Intra particle diffusion)	R^2	0.9327	0.9575	0.9751
	K_{wm} (mg/g.$min^{0.5}$)	0.0284	0.0298	0.0268
	C (mg/g)	0.4204	0.8499	1.2399
Dumwald Wagner	R^2	0.8345	0.7127	0.4518
	K (L/min)	0.0138	0.0177	0.0187
Banghams	R^2	0.7962	0.8589	0.9568
	K_B	5.6337	6.7748	7.0193
	Θ	0.001	0.0006	0.0004

Vermeulin	R^2	0.8345	0.7127	0.4518
	K_v	0.0139	0.0176	0.0187

The removal of bromothymol blue was studied at different temperatures viz. 313K, 323K and 333K by keeping other parameters constant for the determination of thermodynamic parameters. The thermodynamic parameters the standard enthalpy (ΔH˚), standard free energy (ΔG˚), and standard entropy (ΔS˚) are considered to characterize the adsorption process due to the transfer of one mole of solute from the solution onto solid–liquid interface [29].

The parameters were determined by the plot of ln K_d against 1/T (Figure 8) the partitioning coefficient K_d (L/mol) of the bromothymol blue towards the biocomposite mix is an important parameter for examining the bromothymol blue molecule migration through the biocomposite mix. The values of the ΔG˚ estimated in Table 9 are positive for all three temperatures studied at various contact time studied. The was observed that ΔG˚ parameters in Table 9 were all positive and increases with increase with temperature for all contact time studied. The exothermic nature is indicated by the decrease in the amount of adsorption with temperature. The value of Δ*H*, Δ*S* and Δ*G* result shows that the process was exothermic, non-spontaneous and thermodynamically not feasible. The negative value of ΔS° shows the decreasing randomness at the solid/liquid interface during the sorption of bromothymol blue dye onto biocomposite mix of *G. sepium* and *Acacia* pod.

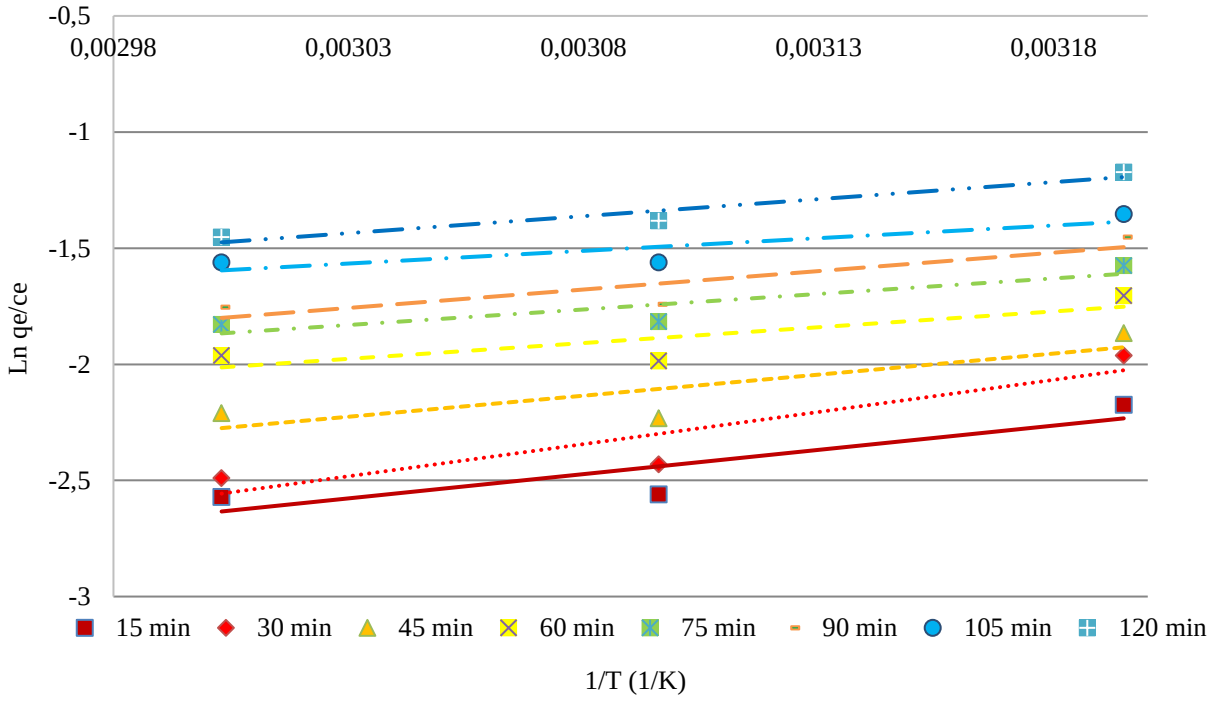

Figure 8. Vant Hoff's plot the biosorption of bromothymol blue onto the biocomposite mix

Table 9. Estimated thermodynamic parameter for the removal of bromothymol blue onto *Gliricidia sepium* ad *Acacia* pod biocomposite.

Time (mins)	Temperature (K)	K_d	Ln K_d	ΔG (J/mol)	ΔH (J/mol)	ΔS (J/mol.K)
15	313	0.1137	-2.1745	5658.7	-17368.8	-74.0545
	323	0.0773	-2.5598	6976.7		
	333	0.0764	-2.5716	7119.6		
30	313	0.1406	-1.9621	5105.9	-23011.5	-90.3566
	323	0.0880	-2.4307	6729.5		
	333	0.0880	-2.4892	6684.6		
45	313	0.1548	-1.8655	4854.6	-15073.3	-64.1774
	323	0.1073	-2.2328	5996.0		
	333	0.1098	-2.2095	6117.1		
60	313	0.1820	-1.7039	4434.0	-11320.3	-50.7337
	323	01372	-1.9860	5333.2		
	333	0.1406	-1.9621	5432.2		
75	313	0.2071	-1.5744	4097.0	-11124.1	-48.9279
	323	0.1626	-1.8165	4878.1		
	333	0.1606	-1.8288	5063.2		
90	313	0.2340	-1.4525	3779.8	-13198.5	-54.6022
	323	0.1752	-1.7418	4877.5		
	333	0.1730	-1.7544	4857.2		
105	313	0.2583	-1.3535	3443.3	-9083.9	-40.5441
	323	0.2099	-1.5611	4192.2		
	333	0.2099	-1.5611	4322.2		
120	313	0.3095	-1.1727	3051.7	-12181.7	-48.8431
	323	0.2510	-1.3822	3711.8		
	333	0.2340	-1.4525	4021.3		

4. CONCLUSIONS

The biocomposite developed by modification of *G. sepium* (A) and *Acacia* pod (B) with 0.1M of diluted H_2O_2 (1: 100) of different biocomposite mixture ratio of 7 experimental runs as suggested by the design expert software. The most effective run that gave the highest adsorption capacity and removal efficiency is Run 3 (0.95A: 0.05B). Two-Level factorial design in the Design of Expert was an appropriate tool to evaluate the quality of the model which gave R^2 to be 0.9999 and 0.9851 for adsorption capacity and removal efficiency respectively. The FTIR used for suggesting the surface chemistry of the *G. sepium* and *Acacia* pods indicate the large presence of O-H, C-O, N-H and C=C and there was appearance and disappearance of the O-H stretch, C=O, C-Cl, C-F, $c \equiv c$ stretch groups in the untreated and treated *G. sepium* pod at different peaks, while appearance of C-H, C-Cl, O-H, N-H bend and $c \equiv c$ stretch groups where noticed in the treated and untreated *Acacia* pod at different peaks.

The effect of initial concentration studied showed an increase in adsorption capacity with time and also increases with increasing initial concentration. Removal efficiency was observed for the varying concentration of the dye gave an increase in adsorption capacity and removal efficiency as concentration was increased from 10 mg/l to 20 mg/l. The equilibrium data fitted best to the Freundlich and Temkin isotherms model. The pseudo-first-order model, pseudo-second-order model, and Elovich model were studied on the kinetic of the adsorption but the pseudo-second order as well as the Elovich models were observed to be suitable for the design of kinetic model as they show a better fit compared to the Pseudo-first order. The mechanism of the adsorption was controlled by Weber - Morris ($intra-particle$) diffusion model showing that pore diffusion and boundary layer diffusion controlled the adsorption to some degree. The adsorption process is heterogeneous, exothermic, non-spontaneous and decreased randomness on solid/solute interface for the biocomposite developed.

It can be deduced that *G. sepium* and *Acacia* pod are effective agricultural materials for the development of a biocomposite as adsorbent in adsorption study due to its high yield, good adsorption capacity, removal efficiency and increase in rate of adsorption. These properties make *G. sepium* and *Acacia* pod adsorbents a huge potential in remediating spent dyes in textile industries. In conclusion, effect of initial concentration of the adsorbate has a great influence in the adsorption.

Acknowledgement

We thank the Bioenvironmental Water and Engineering Research group (BWERG), Department of Chemical Engineering, Ladoke Akintola University of Technology, Ogbomoso, Oyo state, Nigeria.

References

[1] Karuna, S., Pankaj, K., & Rajani, S. (2017, January). An Overview of Textile Dyes and their Removal Techniques: Indian Perspective. *Journal of Pollution Research*, 36(4), 790-797

[2] Adegoke, A. K., & Bello, S. O. (2015, December). Dye Sequestration Using Agricultural Waste as Adsorbents. *Water Resources and Industry*, 12, 8-24

[3] Orts, F., Rio, D., Molina, J., Bonastre, J., & Cases, F. (2018). Electrochemical Treatment of Real Textile Wastewater: Trichromy Procion HEXL. *Journal of Electroanalytical Chemistry*, 808, 387-394

[4] Jordao, C., Puppim, R., & Broega, A. (2018). Solution Notes on Clean Textile Waste. *Internation Conference on Innovation, Engineering and Entrepreneurship* (pp. 682-689). Cham: Springer.

[5] Sabino De Gisi, Giusy Lofrano, Mariangela Grassi, Michele Notarnicola, Characteristics and adsorption capacities of low-cost sorbents for wastewater treatment: A review. *Sustainable Materials and Technologies,* Volume 9, 2016, Pages 10-40, https://doi.org/10.1016/j.susmat.2016.06.002

[6] Qadeer, R. (2007). Adsorption Behavior of Ruthenium Ions on Activated Charcoal from Nitric Acid Medium, Colloids Surf. A. *Physiochem. Eng. Asp.* 293, 217-223

[7] Okeowo, I. O., Balogun, E. O., Ademola, A. J., Alade, A. O., Afolabi, T. J., Dada, E. O., & Farombi, A. G. (2020). Adsorption of phenol from wastewater using microwave-assisted Ag–Au nanoparticle-modified mango seed shell-activated carbon. *International Journal of Environmental Research*, 14(2), 215-233

[8] Bhattacharya, A., Naiya, T., Mandal, S., & Das, S. (2008). Adsorption, Kinetics and Equilibrium Studies on Removal of Cr(VI) from Aqueous Solutions using Different Low cost adsorbents. *Chemical Engineering Journal*, 137, 529-541

[9] Hegazy, S. K., Mabrouk, M. M., Elsisi, A. E., & Mansour, N. O. (2012). Effect of clarithromycin and fluconazole on the pharmacokinetics of montelukast in human volunteers. *European Journal of Clinical Pharmacology*, 68(9), 1275-1280

[10] Halder, G., Dhawane, S., Barai, P. K., & Das, A. (2015). Optimizing chromium (VI) adsorption onto superheated steam activated granular carbon through response surface methodology and artificial neural network. *Environmental Progress & Sustainable Energy*, 34(3), 638-647

[11] Dixit, R., Malaviya, D., Pandiyan, K., Singh, U. B., Sahu, A., Shukla, R., & Paul, D. (2015). Bioremediation of heavy metals from soil and aquatic environment: an overview of principles and criteria of fundamental processes. *Sustainability*, 7(2), 2189-2212

[12] Olajire, A., Abidemi, J., Lateef, A., & Benson, N. (2017). Adsorptive desulphurization of model oil by Ag nanoparticles- modified activated carbon prepared from brewer's spent grains. *Journal of Environment Chemical Engineering*, 5, 147-159

[13] Latinwo, G., Jimoda, L., & Agarry, S. (2015). Biosorption of some heavy metals from textile wastewater by green seaweed biomass. *Universal Journal of Environmental Research & Technology*, 5(4), 210-219.

[14] Langmuir, I. (1918). The adsorption of gases on plane surfaces of glass, mica and platinum. *Journal of the American Chemical Society*, 40(9), 1361-1403

[15] Johnson, R. D., & Arnold, F. H. (1995). The Temkin isotherm describes heterogeneous protein adsorption. *Biochimica et Biophysica Acta (BBA) - Protein Structure and Molecular Enzymology*, 1247(2), 293-297

[16] Hammud, H. (2011, December). Biosorption Studies of Methylene Blue by Mediterranean AlgaeCarolina and Its Chemically Modified Fornis. Linear and Nonlinear Models' Prediction Based on Statistical Error Calculation. *Intonational Joumal of Chemistry*, 3(4), 147-163

[17] Saikaew, W., Kaewsarn, P., & Saikaew, W. (2009). Pomelo Peel: Agricultural Waste for Biosorption of Cadmium Ions from Aqueous solution. *World Acad. Sci. Eng. Technol.* 56, 287-290

[18] Başar, C. A. (2006). Applicability of the various adsorption models of three dyes adsorption onto activated carbon prepared waste apricot. *Journal of Hazardous Materials*, 135(1-3), 232-241

[19] Gupta, V. K., Pathania, D., Sharma, S., Agarwal, S., & Singh, P. (2013). Remediation of noxious chromium (VI) utilizing acrylic acid grafted lignocellulosic adsorbent. *Journal of Molecular Liquids*, 177, 343-352

[20] Dada, A. O., Olalekan, A. P., Olatunya, A. M., & Dada, O. J. I. J. C. (2012). Langmuir, Freundlich, Temkin and Dubinin–Radushkevich isotherms studies of equilibrium sorption of Zn2+ unto phosphoric acid modified rice husk. *IOSR Journal of Applied Chemistry*, 3(1), 38-45

[21] Azizian, S. (2004). Kinetic models of sorption: a theoretical analysis. Journal of colloid and Interface Science, 276(1), 47-52

[22] Ho, Y. S., & McKay, G. (1999). Pseudo-second order model for sorption processes. *Process Biochemistry*, 34(5), 451-465

[23] Wu, F. C., Tseng, R. L., & Juang, R. S. (2009). Characteristics of Elovich equation used for the analysis of adsorption kinetics in dye-chitosan systems. *Chemical Engineering Journal*, 150(2-3), 366-373

[24] Sulthana, R., Taqui, S. N., Zameer, F., Syed, U. T., & Syed, A. A. (2018). Adsorption of ethidium bromide from aqueous solution onto nutraceutical industrial fennel seed spent: kinetics and thermodynamics modelling studies. *International Journal of Phytoremediation*, 20(11), 1075-1086

[25] Wu, F. C., Tseng, R. L., & Juang, R. S. (2009). Initial behaviour of intraparticle diffusion model used in the description of adsorption kinetics. *Chemical Engineering Journal*, 153(1-3), 1-8

[26] Reddy, E., Banote, R., Chatti, K., Kulkarni, P., & Rajadurai, M. (2012). Selective Multicolour Imaging of Zebrafish Muscle Fibres by Using Fluorescent Organic Nanoparticles. *Chembiochem: A European Journal of Chemical Biology*, 13(13), 1889-1894

[27] Bangham, A. D., Hill, M. W., & Miller, N. G. A. (1974). Preparation and use of liposomes as models of biological membranes. In Methods in membrane biology (pp. 1-68). Springer, Boston, MA.

[28] Miyauchi, T., & Vermeulen, T. (1963). Diffusion and back-flow models for two-phase axial dispersion. *Industrial & Engineering Chemistry Fundamentals*, 2(4), 304-310

[29] Bello, O., Bello, O., & Lateef, I. (2014, June). Adsorption characteristics of mango leaf (mangifera Indica) as adsorbent for malachite green dye removal fron aqueous solution. *Covenant Journal of Physical and Life Sciences* 2(1), 1-13

[30] H. M. F. Freundlich, Over the Adsorption in Solution. *The Journal of Physical Chemistry*, Vol. 57, 1906, pp. 385-471